

This is a repository copy of *Analysis of plasma enhanced pulsed laser deposition of transition metal oxide thin films using medium energy ion scattering*.

White Rose Research Online URL for this paper:
<https://eprints.whiterose.ac.uk/132771/>

Version: Accepted Version

Article:

Rossall, Andrew K. orcid.org/0000-0002-0123-8163, van den Berg, Jaap A., Meehan, David et al. (2 more authors) (2019) Analysis of plasma enhanced pulsed laser deposition of transition metal oxide thin films using medium energy ion scattering. Nuclear Instruments and Methods in Physics Research Section B: Beam Interactions with Materials and Atoms. pp. 274-278. ISSN 0168-583X

<https://doi.org/10.1016/j.nimb.2018.06.023>

Reuse

This article is distributed under the terms of the Creative Commons Attribution-NonCommercial-NoDerivs (CC BY-NC-ND) licence. This licence only allows you to download this work and share it with others as long as you credit the authors, but you can't change the article in any way or use it commercially. More information and the full terms of the licence here: <https://creativecommons.org/licenses/>

Takedown

If you consider content in White Rose Research Online to be in breach of UK law, please notify us by emailing eprints@whiterose.ac.uk including the URL of the record and the reason for the withdrawal request.

Analysis of plasma enhanced pulsed laser deposition of transition metal oxide thin films using medium energy ion scattering

Andrew K. Rossall*, Jaap A. van den Berg

School of Computing and Engineering, University of Huddersfield, Queensgate, Huddersfield, HD1 3DH, UK

David Meehan, Sudha Rajendiran, Erik Wagenaars

York Plasma Institute, Department of Physics, University of York, York, YO10 5DD, UK

Abstract

In this study, plasma-enhanced pulsed laser deposition (PE-PLD), which is a novel variant of pulsed laser deposition that combines laser ablation of metal targets with an electrically-produced oxygen plasma background, has been used for the fabrication of ZnO and Cu₂O thin films. Samples prepared using the PE-PLD process, with the aim of generating desirable properties for a range of electrical and optical applications, have been analysed using medium energy ion scattering. Using a 100 keV He⁺ ion beam, high resolution depth profiling of the films was performed with an analysis of the stoichiometry and interface abruptness of these novel materials. It was found that the PE-PLD process can create stoichiometric thin films, the uniformity of which can be controlled by varying the power of the inductively coupled plasma. This technique showed a high deposition rate of $\sim 0.1 \text{ nm s}^{-1}$.

Keywords: Medium energy ion scattering, nano-layer profiling, plasma-enhanced pulsed laser deposition, thin film, transition metal oxide, inductively coupled plasma.

1. Introduction

Transition metal oxides can behave as insulators, semiconductors or metals and can undergo semiconductor-metal transitions making them attractive candidates for future functional devices due to their many switchable physical properties [1, 2, 3]. The unusual (and often useful) properties are largely determined by the unique nature of the outer d-electrons of the transition metal (TM) ions arising from flexible valence states.

Over the past decade or so, there has been a significant expansion of research into the production of transition metal oxide (TMO) thin films for use as inorganic functional materials in a range of electrical, optical and magnetic applications. Some of these potential applications include electrodes in chemical processes, catalytic processing, gas sensors, high density memories, passive display electrodes, fuel cells and micro electronic circuits, to name a few.

Well controlled fabrication of these thin films can be challenging due to the requirement for efficient stoichiometric mass transfer, high deposition rates and well defined interfaces between layers. Techniques such as chemical vapour deposition, molecular beam epitaxy, magnetron plasma sputtering and pulsed laser deposition (PLD) have all been used successfully to fabricate TMO thin films with some desirable properties [4]. The PLD technique has the advantage of high deposition rates, a degree of control over stoichiometry and the capability to overcome the high melting points for many of the TMOs. Disadvantages include a limited area of deposition and the possible incorporation of macroscopic particles in the films [5]. In the

*Corresponding author

Email address: a.rossall@hud.ac.uk (Andrew K. Rossall)

work reported here, an extension of the PLD technique is examined, which incorporates an inductively coupled low temperature oxygen plasma into the PLD process and is known as plasma enhanced PLD (PE-PLD). The reactive oxygen plasma interacts with the pure TM ablation plume, effectively de-coupling the formation of the reactive oxygen species and the transition metal ions. Through careful control of the plasma parameters, i.e. pressure, power, bias and discharge geometry, the quantities of the different reactive species can be controlled. This control over the reactive species present can then be optimised for stoichiometry control and crystal structure growth of the film.

Films produced by PE-PLD were analysed using the Medium Energy Ion Scattering (MEIS) facility at the University of Huddersfield in terms of the composition and nano-layer structure of the thin films. Thin films of ZnO and Cu₂O have been deposited on quartz substrates using the PE-PLD system newly set-up at the York Plasma Institute (YPI) at the University of York [6]. Experimental results are presented and compared to simulations of the MEIS energy spectra followed by a discussion outlining the effect of the plasma parameters on the deposited thin films.

2. Experimental Set-up

2.1. Plasma enhanced pulsed laser deposition

Plasma Enhanced-Pulsed Laser Deposition (PE-PLD) is able to create oxide thin films by the interaction between two separate plasmas. Firstly, an oxygen Inductively Coupled Plasma (ICP) is created within a Gaseous Electronics Conference (GEC) reference cell [7], with a grounded bottom electrode, and a top quartz electrode housing a planar coil, connected via matching unit to a radio frequency power supply (Advanced Energy Caesar 1310, 1 kW 13.56 MHz). A vacuum vessel houses the ICP, and is initially pumped down to high vacuum ($< 10^{-4}$ Pa) after which pure oxygen is let in until the desired pressure (typically 3 to 25 Pa) is reached, controlled by a mass flow controller (MKS Instruments). The discharge geometry is shown schematically in figure 1.

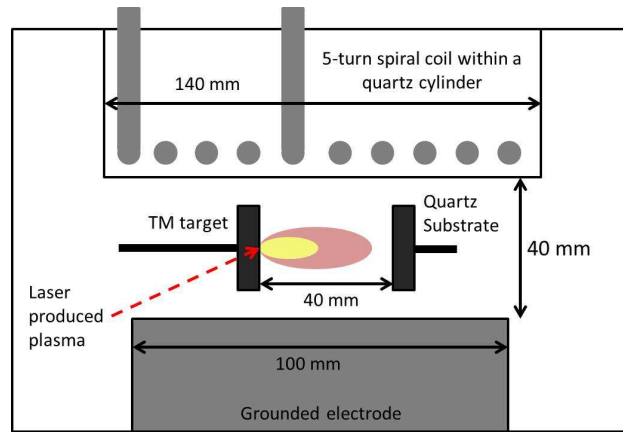


Figure 1: Schematic diagram of the inductively coupled plasma source with the laser produced plasma. The reactor is cylindrically symmetric and consists of a stainless steel vacuum chamber, a 5-turn coil antenna inside a quartz cylinder, and a metal electrode. The design is based on the GEC rf reference cell [7, 8].

Secondly, a metal target, mounted on a rotatable stage that can be controlled manually from outside the chamber, is ablated within the GEC cell. The target is ablated using a q-switched Continuum Minilite Nd:YAG laser of 532 nm wavelength, 35 mJ per pulse, 5 ns pulse length and 10Hz pulse rate, which is focused to 1 mm focal diameter on target.

It is the reaction between the plasma from the ablated metal target, and the reactive oxygen species created by the ICP, that results in a deposition of a metal oxide thin film on a quartz substrate, which was cleaned with isopropanol in an ultrasonic bath prior to deposition. The substrate is mounted on a fixed, unheated mount, 40 mm away from the target within the ICP.

1
2
3
4
50 The oxygen ICP is pulsed at 10 Hz in order match the repetition rate of the laser and to maintain a
5 low gas temperature. The timing of the plasma power and laser is controlled by an external digital delay
6 generator (Stanford Instruments). The plasma is ignited and allowed to reach equilibrium, 8 ms later the
7 laser flash lamp is powered and after a further 150 μ s the laser triggered. After a total of 10 ms, power is no
8 longer applied to the plasma, which allows 2 ms for the plasma plume to fully propagate to the substrate.

9 10 *2.2. Medium energy ion scattering*

11 The MEIS Facility uses H^+ and He^+ ions with energies between 50 - 200 keV to provide high resolution
12 depth profiling of crystalline and non-crystalline nanometre thin layers [9]. Medium energy ion scattering
13 is a lower energy variant of Rutherford Back Scattering (RBS) with enhanced depth resolution due to the
14 use of a high resolution toroidal electrostatic analyser. For this work, He^+ ions impinge onto the TMO thin
15 film samples, losing energy inelastically within the sample via interactions with the electron clouds of the
16 constituent elements. The interaction with the electrons do not impart sufficient momentum to the ion to
60 deflect the projectile and the ion continues on a straight path until a large angle deflection occurs off an
17 atomic core, followed by further inelastic energy loss as the ion exits the sample. By analysing the energy
18 of the ions scattered off the sample at a specific angle, an energy spectrum is produced. A best fit analysis
19 of simulated spectra (see section 3.1), generated using an assumed layer structure, to the experimental
20 data provides a depth profile with near nano-meter resolution, enabling the analysis of layer structure,
21 stoichiometry and interface abruptness.
22

23
24 The parameters for this experiment were 100 keV He^+ ions impinging on the samples at an incident
25 angle of 36° w.r.t. the target surface and a scattering angle of 125° was chosen to maximise mass and
26 energy/depth dispersion. Beam currents ranged between 25 and 40 nA and the dose received on target was
27 controlled using a current integrator measuring a fraction of the ion current at the entrance port of the
70 scattering chamber.
28
29

30 *2.3. Energy dispersive X-ray spectroscopy*

31 Energy dispersive X-ray (EDX) spectroscopy was carried out at the York JEOL Nanocentre [10] using
32 their JEOL 7800F Prime high resolution scanning electron microscope (SEM). The JEOL 7800F Prime SEM
33 includes a full EDX chemical microanalysis system with an atmospheric thin window (ATW) detector. The
34 EDX system was used to determine the chemical composition of the surface of the deposited thin films. An
35 energy of 5 keV was used to analyse the copper samples and an energy of 3 keV for the zinc samples. The
36 EDX has a working distance of 10 mm and the detector is $\sim 40^\circ$ from the plane of the target surface.
37
38

39 **3. Simulation**

40
41 A complete description of the models and software used to simulate the generation of the reactive oxygen
42 plasma species and the laser ablation plume formation and propagation have been previously reported [5].
43

44 *3.1. MEIS spectrum simulation*

45 The simulation model used operates as a macro within the IGOR[®] graphing and data analysis package
46 [11]. The program was originally developed at Daresbury Laboratory [12] and is now maintained at the
47 University of Huddersfield. The experimental energy spectrum is fitted with a multipoint curve to remove the
48 dechanneling background and an initial depth profile is assumed using knowledge of the deposition technique
49 and the position of the surface peaks in the MEIS spectrum. The software divides the initially assumed
50 concentration depth profile into thin layers (typically 0.1 nm in width) and, using the scattering conditions
51 provided, calculates the scattering contributions from each of these layers. The scattering contributions are
52 represented as Gaussian profiles with heights proportional to the scattering cross-section. Inelastic energy
53 loss is calculated using stopping powers from SRIM [13] with Bragg's rule being used to modify the stopping
54 powers near an interface to account for changing composition (e.g. by interdiffusion or interface roughness).
55 Degradation of the system resolution with depth is accounted for by introducing an amount of straggling
56 for each layer which results in a reduction in slope of the Gaussians with increasing depth. The shallowing
57
58

1
2
3
4 95 of slope observed over and above that which is due to straggling is ascribed to interdiffusion. All layer
5 contributions are added together and the resultant simulated spectrum is compared with the experimental
6 spectrum. The layer structure is then varied iteratively to improve the match between simulation and
7 experiment where the best layer structure is decided by minimising χ^2 for the overall fit.
8

9 4. Results and discussion

10 4.1. PE-PLD parameters

11
12 For this initial study, 3 parameters for the ICP were varied to determine their effect on the deposited
13 TMO thin film. Oxygen pressures of 7.5 and 13 Pa, plasma powers of 500 and 700 W and deposition times
14 of 2.5 and 5 minutes were used. The Nd:YAG laser is incident onto pure Zn and Cu targets with the laser
15 plasma plume propagating through the oxygen ICP before coating the quartz substrate. An oxygen pressure
16 of 7.5 Pa was used to produce the Cu₂O thin films and an oxygen pressure of 13 Pa was used for the ZnO
17 films.
18

19 4.2. Energy dispersive X-ray spectroscopy (EDX)

20
21 ThermoFisher Scientific [14] software was used in conjunction with the JOEL 7800F system to perform
22 the EDX analysis on the ZnO and Cu₂O thin films. The results [15, 16] indicate the stoichiometric depen-
23 dence of the thin films on the oxygen pressure within the chamber. Atomic fractions determined from EDX
24 measurements were compared with those determined from the simulations of the MEIS spectra.
25

26 4.3. Medium energy ion scattering

27
28 Medium energy ion scattering spectra for Cu₂O and ZnO and comparison with simulations (as described
29 in section 3.1) are shown in figures 2 and 3, where the TM peaks are marked. To determine deposition rates,
30 the depth of the layer was taken as the FWHM of the TM peak. From the best fit depth profiles shown
31 alongside the MEIS spectra (see figures 2(b), 2(d), 3(b) and 3(d)), layer thicknesses of 32.4 nm and 13.5
32 nm for Cu₂O and of 37.2 nm and 18.9 nm for ZnO have been determined for deposition times of 5.0 and
33 2.5 minutes respectively. These depth profiles give a deposition rate of $\sim 0.1 \text{ nm s}^{-1}$ and by using a laser
34 operating at 10 Hz, this provides sub-nanometre control over the thickness of deposited layers.
35

36 The oxygen peaks in the MEIS spectra are small due to a lower cross-section for interaction, reducing
37 the accuracy as a result. Results from EDX were used to confirm the stoichiometry of the film and the
38 determined atomic fractions were then compared with the MEIS simulations. The χ^2 fit of the simulated
39 MEIS spectra with the experimental data corroborated the EDX results as shown in figures 2 and 3.

40 An approximately 7% enrichment of the TM is observed in the deepest layer (lowest energy in the peak)
41 when compared to the surface layer as shown in figures 2(a) and 3(a) for the higher plasma power of 700 W.
42 Conversely, an approximately 3% reduction in the Cu signal at the deepest layer and a uniform Zn depth
43 profile is observed with the lower plasma power of 500 W as shown in figure 2(c) and 3(c). This indicates
44 a dependence of thin film uniformity on the plasma power as a similar behaviour is observed with different
45 deposition times and oxygen pressures.
46

47 As deposition time increases, the slope of the silicon surface peak signal originating from the quartz
48 substrate is seen to become more shallow (see figures 2(a), 2(c), 3(a) and 3(c)) indicating increasing interdif-
49 fusion between the TMO thin film layer and the substrate. After 2.5 minutes, the interface region is 46% of
50 the deposited film thickness and after 5.0 minutes the interface region is 38% of the deposited film thickness.
51 The interface region is defined here as the difference in depth between the point at which the atomic fraction
52 of the TM drops by 10% and the point at which the silicon fraction is 10% less than stoichiometric for SiO₂.
53 Depth profiles with indicated interface regions for Cu₂O after 2.5 and 5.0 minutes deposition time are shown
54 in figures 4(a) and 4(b).
55

56 Due to the low energies of the reactive species involved in this technique and the lack of a bias applied
57 to the substrate the large interface region observed using MEIS is likely to have been caused by substrates
58 with an initial high surface roughness parameter (R_a) and then worsened by collisional processes associated
59 with the slow moving molecules. There is a known connection between interdiffusion and surface roughness
60
61
62
63
64
65

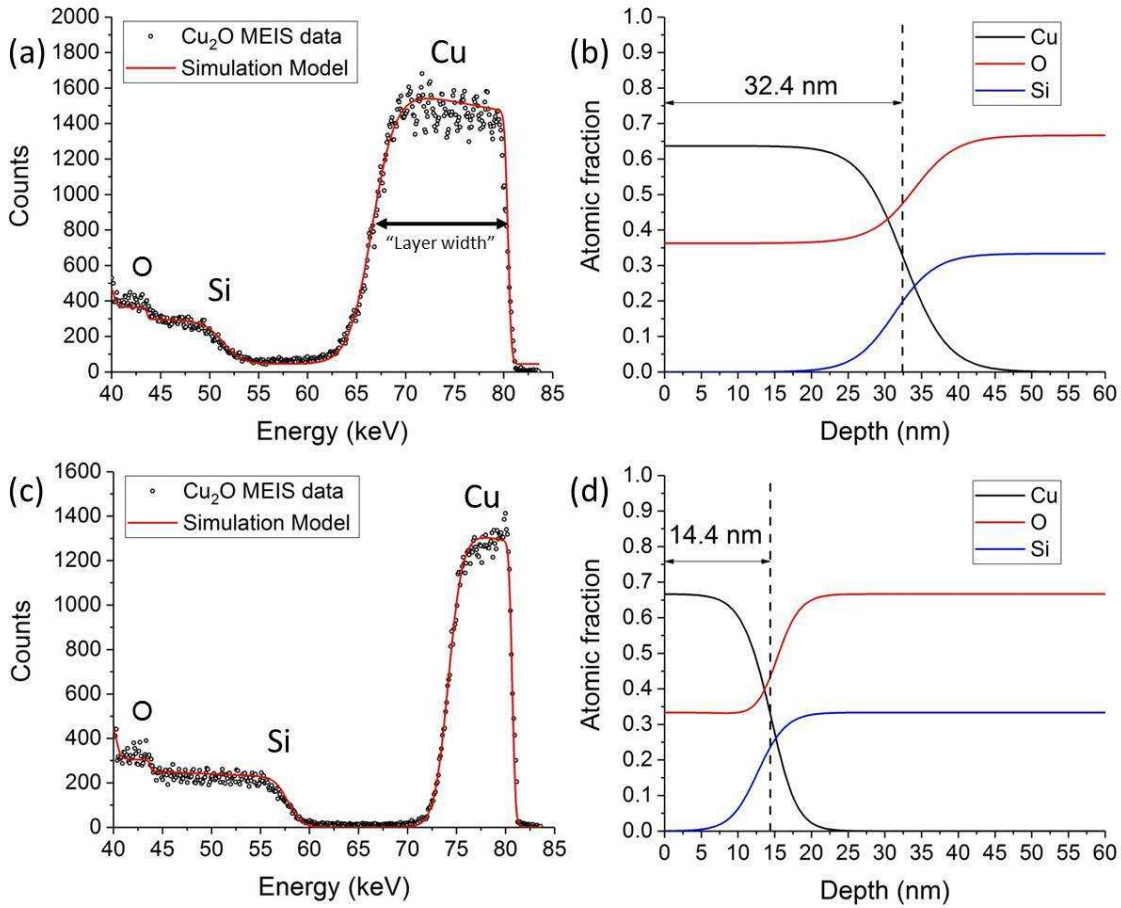


Figure 2: (a) MEIS spectra and comparison to simulation for Cu₂O with corresponding depth profiles (b) for plasma power of 700 W and a deposition time of 5 minutes; and (c) MEIS spectra and comparison to simulation for Cu₂O with corresponding depth profiles (d) for plasma power of 500 W and a deposition time of 2.5 minutes.

[17]. The initial surface condition of the substrate after ultrasonic cleaning is currently undetermined and will be investigated further along with different substrates and substrate preparation procedures.

5. Conclusions

Plasma-enhanced pulsed laser deposition (PE-PLD) has been used to fabricate ZnO and Cu₂O thin films which have been analysed using medium energy ion scattering to examine the uniformity of the thin films and the interface region between the thin film and substrate. The deposited films indicated a larger than expected interface region which is likely due to the initial high surface roughness parameter of the substrate creating a more blended interface which is then worsened via collisional processes.

These initial results demonstrate that the PE-PLD process yields a high deposition rate of 0.1 nm s⁻¹ with sub-nm control over the film thickness. The deposited films are stoichiometric and varying the plasma power has shown to cause enrichment or depletion of the transition metal providing control over the uniformity of the thin film.

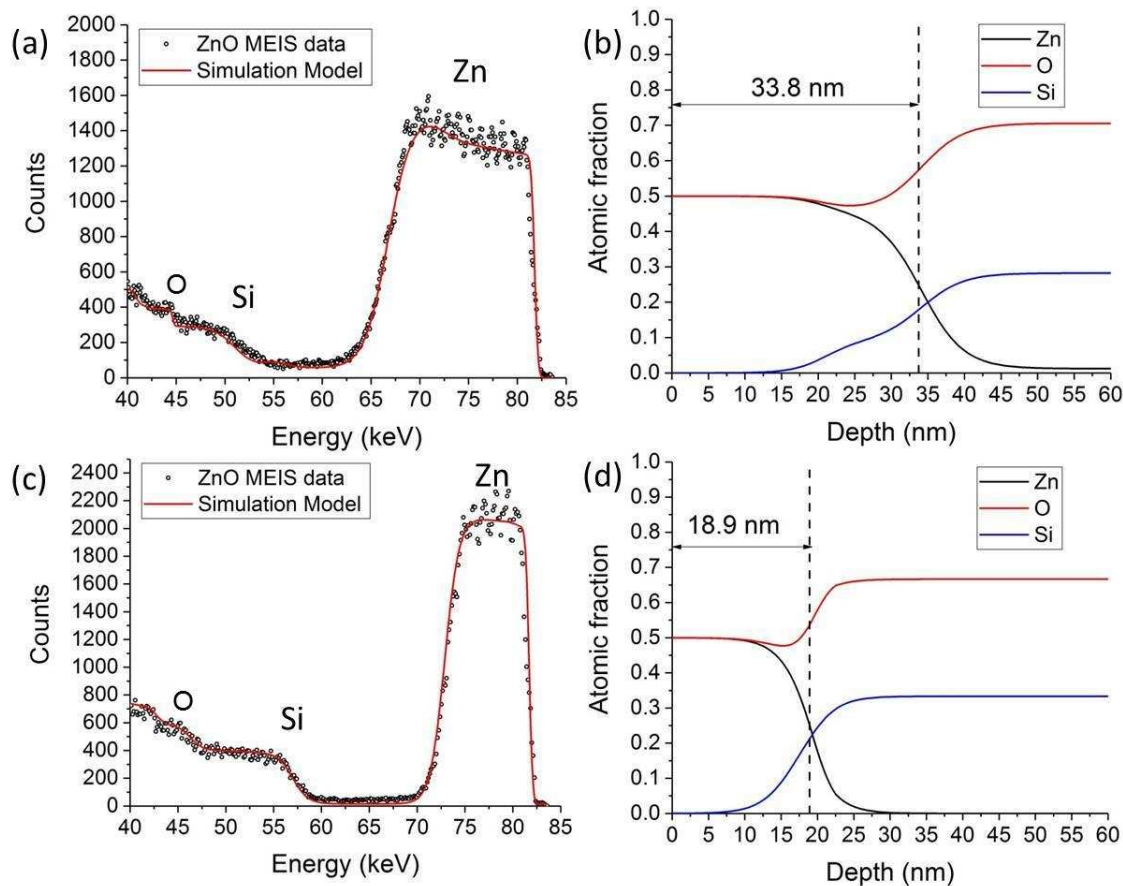


Figure 3: (a) MEIS spectra and comparison to simulation for ZnO with corresponding depth profiles (b) for plasma power of 700 W and a deposition time of 5 minutes; and (c) MEIS spectra and comparison to simulation for ZnO with corresponding depth profiles (d) for plasma power of 500 W and a deposition time of 2.5 minutes.

References

- [1] K. Gesheva, T. Ivanova, G. Bodurov, I. M. Szilgyi, N. Justh, O. Kri, S. Boyadjiev, D. Nagy, M. Aleksandrova, Technologies for deposition of transition metal oxide thin films: application as functional layers in smart windows and photocatalytic systems, *Journal of Physics: Conference Series* 682 (1) (2016) 012011. URL <http://stacks.iop.org/1742-6596/682/i=1/a=012011>
- [2] Y.-C. Liang, Growth and characterization of nonpolar a-plane ZnO films on perovskite oxides with thin homointerlayer, *Journal of Alloys and Compounds* 508 (1) (2010) 158 – 161. doi:<http://dx.doi.org/10.1016/j.jallcom.2010.08.037>. URL <http://www.sciencedirect.com/science/article/pii/S0925838810020189>
- [3] X. Yu, T. J. Marks, A. Facchetti, Metal oxides for optoelectronic applications, *Nature Materials* 15 (4) (2016) 383–396. doi:10.1038/nmat4599. URL <http://www.nature.com/doifinder/10.1038/nmat4599>
- [4] J.-J. Chen, X.-R. Deng, H. Deng, Progress in the growth and characterization of nonpolar ZnO films, *Journal of Materials Science* 48 (2) (2013) 532–542. doi:10.1007/s10853-012-6721-7. URL <https://doi.org/10.1007/s10853-012-6721-7>
- [5] S. Rajendiran, A. Rossall, A. Gibson, E. Wagenaars, Modelling of laser ablation and reactive oxygen plasmas for pulsed laser deposition of zinc oxide, *Surface and Coatings Technology* 260 (2014) 417 – 423. doi:10.1016/j.surfcoat.2014.06.062.
- [6] York Plasma Institute, <https://www.york.ac.uk/physics/yypi/>.
- [7] P. A. Miller, G. A. Hebner, K. E. Greenberg, P. D. Pochan, B. Aragon, An inductively coupled plasma source for the gaseous electronics conference rf reference cell, in: *J. Res. Natl. Inst. Stand. Technol.*, Vol. 100, 1996, pp. 427–427.
- [8] P. J. H. Jr., K. E. Greenberg, P. A. Miller, J. B. Gerardo, J. R. Torczynski, M. E. Riley, G. A. Hebner, J. R. Roberts, J. K.

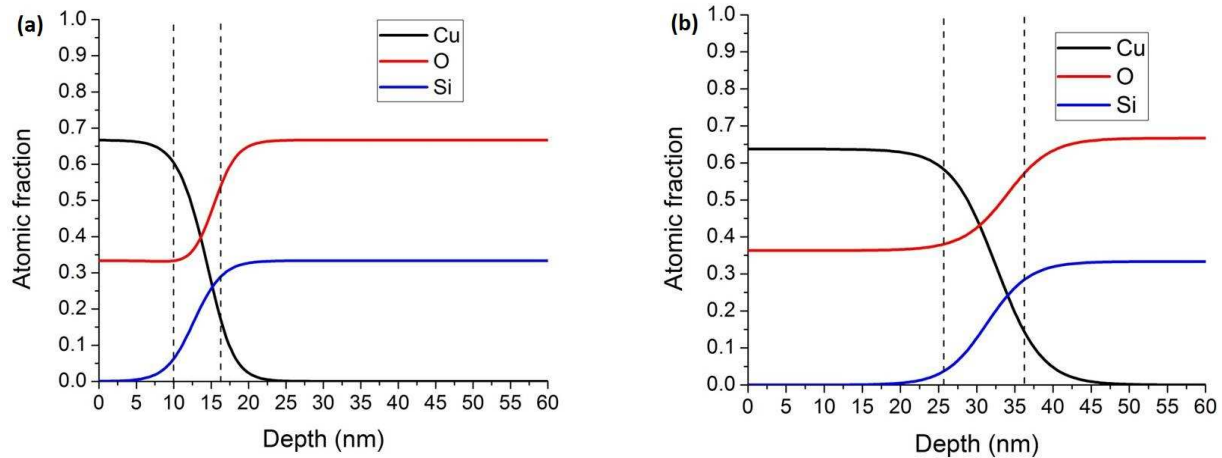


Figure 4: Depth profiles for Cu_2O indicating the size of the interface region between the TMO thin film and the quartz substrate after (a) 2.5 minutes and (b) 5 minutes deposition time.

175 Olthoff, J. R. Whetstone, R. J. V. Brunt, M. A. Sobolewski, H. M. Anderson, M. P. Splichal, J. L. Mock, P. Bletzinger, A. Garscadden, R. A. Gottscho, G. Selwyn, M. Dalvie, J. E. Heidenreich, J. W. Butterbaugh, M. L. Brake, M. L. Pas-sow, J. Pender, A. Lujan, M. E. Elta, D. B. Graves, H. H. Sawin, M. J. Kushner, J. T. Verdeyen, R. Horwath, T. R. Turner, The gaseous electronics conference radiofrequency reference cell: A defined parallelplate radiofrequency system for experimental and theoretical Review of Scientific Instruments 65 (1) (1994) 140–154. arXiv:<http://dx.doi.org/10.1063/1.1144770>, doi:10.1063/1.1144770.

180 URL <http://dx.doi.org/10.1063/1.1144770>

[9] J. van den Berg, M. Reading, P. Bailey, T. Noakes, C. Adelmann, M. Popovici, H. Tielens, T. Conard, S. de Gendt, S. van Elshocht, Medium energy ion scattering for the high depth resolution characterisation of high-k dielectric layers of nanometer thickness, Applied Surface Science 281 (2013) 8–16. doi:10.1016/j.apsusc.2013.02.003.

185 URL <http://www.sciencedirect.com/science/article/pii/S0169433213002961>

[10] The York JEOL Nanocentre, <https://www.york.ac.uk/nanocentre/>.

[11] Wave Metrics Inc., IgorPro. URL <http://www.wavemetrics.com/>

[12] P. Bailey, To be published.

190 [13] J. F. Ziegler, U. Littmark, J. P. Biersack, The stopping and range of ions in solids, Pergamon New York, 1985.

[14] ThermoFisher Scientific, <https://www.thermofisher.com/uk/en/home.html>.

[15] S. Rajendiran, D. Meehan, E. Wagenaars, Phys. Rev. Appl. (In preparation).

[16] D. Meehan, S. Rajendiran, J. Barnard, A. K. Rossall, E. Wagenaars, Plasma enhanced-pulsed laser deposition: proof-of-concept, in: 45th Institute of Physics Plasma Physics Conference, Belfast, UK.

195 [17] A. W. Czanderna, T. E. Madey, C. J. C. J. Powell, Beam effects, surface topography, and depth profiling in surface analysis, Plenum Press, 1998.